A HYBRID ANALYTICAL MODEL FOR ASSESSING THE EFFECT OF RIVER DISCHARGE ON TIDAL DAMPING, APPLIED TO THE MODAOMEN ESTUARY

Huayang Cai[1], Hubert H. G. Savenije[2], Marco Toffolon[3]

Abstract

In this paper we present an analytical approach for assessing the effect of river discharge on tidal dynamics in convergent estuaries. The analytical model makes use of a hybrid analytical expression for tidal damping derived by subtracting the envelopes of high water and low water, using a new approximation of the friction term. The analytical solutions are compared with observations in the Modaomen estuary in China and proved to be both efficient and accurate, suggesting that the proposed model is a powerful analytical instrument for conducting impact assessments induced by human interventions (e.g., flow reduction). The application to the Modaomen demonstrates that the effect of river discharge on tidal dynamics is significant in the upper part of the estuary, where the ratio of river flow to tidal flow amplitude is substantial. The analytical model is able to reproduce the main tidal dynamics with realistic roughness values in the upper part of the estuary, while a model with negligible river discharge only fits observations with unrealistically high roughness values.

Key words: tidal dynamics, envelope method, analytical model, convergent estuary

1. Introduction

Over the last decades there has been an increasing concern about flow reduction in estuaries as a result of human activities, such as dam construction and fresh water withdrawal, which may result in negative effects on the aquatic environment of an estuary and the potential use of water resources. In addition, these anthropogenic interventions have a direct impact on the salt intrusion and storm surge propagation into an estuary. Hence, it is important to understand the effect of river discharge on tidal dynamics. In recent years, impact studies have generally been done by the use of numerical models. While the implementation of such models undoubtedly provides increasingly accurate predictions, they require a lot of time and human resources to develop and are very data intensive. On the contrary, analytical tools can offer a more efficient way of assessing the impact of such interventions. Moreover, they provide direct insights into cause-effect relations. Consequently, the purpose of this study is to provide an analytical instrument for assessing the effect of river discharge on tidal damping in estuaries.

Several papers have discussed analytical methods to analyse the interaction of river discharge and tide in estuaries (Dronkers, 1964; Leblond, 1978; Godin, 1985, 1999; Jay, 1991; Kukulka and Jay, 2003; Horrevoets et al., 2004; Buschman et al., 2009; Jay et al., 2011; Cai et al. , 2012b). Of these, most authors used perturbation analysis, where scaled equations are simplified by neglecting higher order terms, generally neglecting the advective acceleration term and linearising the friction term. Others used a regression model to determine the relationship between river discharge and tide. Exceptions are the approaches by Horrevoets et al. (2004) and Cai et al. (2012b), who provided analytical solutions accounting for river discharge, based on the envelope method originally developed by Savenije (1998).

Recently, Cai et al. (2012a) proposed a new analytical framework for understanding the tidal damping in estuaries. They concluded that the main differences between the examined models (e.g., Savenije et al., 2008; Toffolon and Savenije, 2011; van Rijn, 2011) lies in the treatment of the friction term in the momentum equation. Furthermore, Cai et al. (2012a) presented a new 'hybrid' expression for tidal

[1]Department of Water Management, Delft University of Technology, Netherlands. h.cai@tudelft.nl
[2]Department of Water Management, Delft University of Technology, Netherlands. h.h.g.savenije@tudelft.nl
[3]Department of Civil, Environmental and Mechanical Engineering, University of Trento, Italy. marco.toffolon@unitn.it

damping as a weighted average of the linearized and fully nonlinear friction term. However, they did not include river discharge in that study. In this paper we do include the effect of river discharge on tidal dynamics, making use of the work by Cai et al. (2013) who compared different approaches for the accounting of river discharge on tidal damping. Here we summarize the hybrid approach and illustrate it with an application to the Modaomen estuary.

2. Formulation of the problem

We consider a tidal channel with varying width and depth and investigate the propagation of the tidal wave along an estuary with a fixed bed, where the flow is mainly concentrated in a rectangular cross section, with a possible presence of lateral (intertidal) storage areas, described by the storage width ratio $r_s = B_s / \overline{B}$, i.e., the ratio between the storage width B_s and the stream width $\overline{B}$ (hereafter overbars denote tidal averages).

A sketch of the geometry of the idealized tidal channel is described in Figure 1, together with a simplified picture of the periodic oscillations of water level and velocity defining the phase lag. The basic assumption we made is that the tidally averaged cross-sectional area in alluvial estuaries can be described by an exponentially decreasing function (e.g., Savenije, 1998)

$$\overline{A} = \overline{B}\overline{h} = \overline{A_0} \exp\left(-x / a\right), \tag{1}$$

where x is the longitudinal coordinate directed landward, $\overline{h}$ is the tidally averaged depth of flow, $\overline{A_0}$ is the cross sectional area at the mouth of the estuary and a is the convergence length of the cross-sectional area.

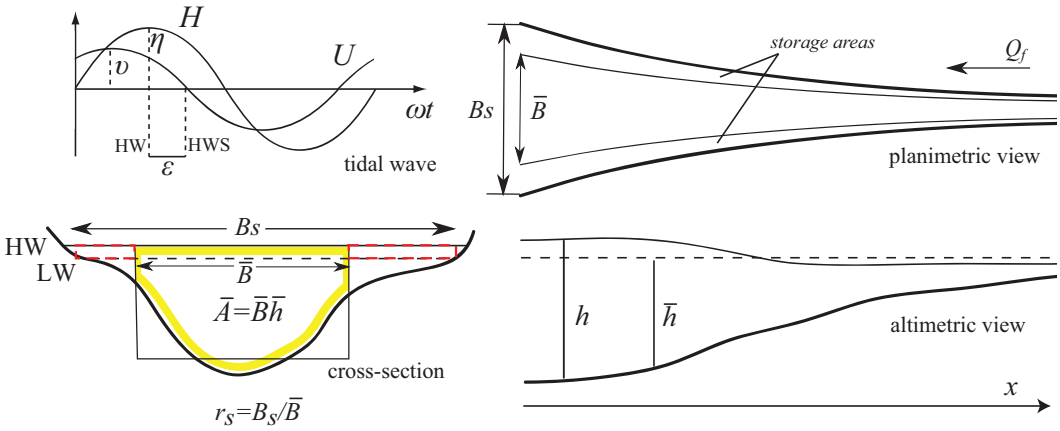

Figure 1. Sketch of the estuary and basic notations.

The one-dimensional hydrodynamic equations in an alluvial estuary are given by (e.g., Savenije, 2005):

$$\frac{\partial U}{\partial t} + U\frac{\partial U}{\partial x} + g\frac{\partial h}{\partial x} + gI_b + gF + \frac{gh}{2\rho}\frac{\partial \rho}{\partial x} = 0, \tag{2}$$

$$r_s\frac{\partial h}{\partial t} + U\frac{\partial h}{\partial x} + h\frac{\partial U}{\partial x} + \frac{hU}{\overline{B}}\frac{\partial \overline{B}}{\partial x} = 0, \tag{3}$$

where t is the time, U is the cross-sectional average flow velocity, h is the flow depth, g is the gravitational acceleration, I_b is the bottom slope, ρ is the water density, H is the free surface elevation, and F is the friction term, defined as:

$$F = \frac{U|U|}{K^2 h^{4/3}}, \tag{4}$$

where K is the Manning-Strickler friction coefficient.

It should be noted that the water level variation $H = h - \bar{h}$. In the case of small tidal amplitude wave, it is possible to find:

$$U\frac{\partial h}{\partial x} = U\frac{\partial\left(H+\bar{h}\right)}{\partial x} = U\frac{\partial H}{\partial x} + \frac{\bar{h}U}{\bar{h}}\frac{\partial \bar{h}}{\partial x} \approx U\frac{\partial H}{\partial x} + \frac{hU}{\bar{h}}\frac{\partial \bar{h}}{\partial x}. \tag{5}$$

where the last step only applies for small value of $H/\bar{h}$.

Substituting equation (5) into (3) and making use of equation (1), the following equation is obtained:

$$r_S\frac{\partial H}{\partial t} + U\frac{\partial H}{\partial x} + h\frac{\partial U}{\partial x} - \frac{hU}{a} = 0, \tag{6}$$

which has the advantage that the depth convergence is implicitly taken into account by the convergence of the tidally averaged cross-sectional area.

The system is forced by a harmonic tidal wave with an amplitude η, a tidal period T, a frequency $\omega=2\pi/T$ and a phase ϕ_H at the mouth of estuary. For the case of a simple harmonic wave with river discharge, the instantaneous flow velocity U is made up of a steady component U_r, created by the discharge of freshwater, and a time-dependent component U_t, contributed by the tide:

$$U = U_t - U_r, \quad U_t = \upsilon\cos\left(\omega t - \phi_U\right), \quad U_r = Q_f/\bar{A}, \tag{7}$$

where Q_f is the freshwater discharge, υ is the amplitude of the tidal velocity and ϕ_U is the phase of tidal velocity.

It is shown that the estuarine hydrodynamics are controlled by a few dimensionless parameters derived for the case of negligible river discharge (Toffolon et al., 2006; Savenije et al., 2008; Toffolon and Savenije, 2011; Cai et al., 2012a). Table 1 presents these independent dimensionless parameters that depend only on the geometry and on the external forcing, i.e., ζ the dimensionless tidal amplitude (indicating the seaward boundary condition), γ the estuary shape number (representing the effect of cross-sectional convergence) and χ the friction number (describing the role of the frictional dissipation), where c_0 is the classical wave celerity of a frictionless progressive wave in a constant-width channel and f is the dimensionless friction factor resulting from the envelope method (Savenije, 1998), defined as:

$$f = \frac{g}{K^2\bar{h}^{1/3}}\left[1-\left(\frac{4}{3}\zeta\right)^2\right]^{-1}, \tag{8}$$

where the factor 4/3 stems from a Taylor approximation of the exponent of the hydraulic radius in the friction term.

Table 1. The definition of dimensionless parameters.

Dimensionless parameters	
Independent	Dependent
Tidal amplitude $\zeta = \eta/\bar{h}$ Estuary shape $\gamma = c_0/(\omega a)$ Friction number $\chi = r_S f c_0 \zeta/(\omega\bar{h})$	Damping number $\delta = c_0 \mathrm{d}\eta/(\eta\omega \mathrm{d}x)$ Velocity number $\mu = \upsilon/(r_S\zeta c_0) = \upsilon\bar{h}/(r_S\eta c_0)$ Celerity number $\lambda = c_0/c$ Phase lag $\varepsilon = \pi/2 - (\phi_H - \phi_U)$

The dependent dimensionless variables are also presented in Table 1, where δ is the damping number (a dimensionless description of the increase, δ>0, or decrease, δ<0, of the tidal wave amplitude along the estuary), μ the velocity number (the actual velocity scaled with the frictionless value in a prismatic channel), λ the celerity number (the ratio between the theoretical frictionless celerity in a prismatic channel and the actual wave celerity) and ε the phase lag between high water (HW) and high water slack (HWS) or between low water (LW) and low water slack (LWS) (for a simple harmonic wave $\varepsilon = \pi/2 - (\phi_H - \phi_U)$) (Toffolon et al., 2006, Savenije et al., 2008).

3. Analytical model for tidal wave propagation

3.1. *Hybrid model with negligible river discharge*

In the case of negligible river discharge, Cai et al. (2012a) showed that the combination of the traditional linear approach (e.g., Toffolon and Savenije, 2011) and the Lagrangean treatment of the friction term by the envelope method (Savenije, 2012; pp.59-94) allows for the best predictive results (we will term this the hybrid model). In particular, the hybrid friction term is the combination of the linearized and the nonlinear Lagrangean friction term, with the optimum weight of the linearized friction term being 1/3, and 2/3 of the nonlinear friction term:

$$F_H = \frac{1}{3}F_L + \frac{2}{3}F = \frac{1}{3}\frac{8}{3\pi}\frac{v}{K^2 h^{4/3}}U + \frac{2}{3}\frac{U|U|}{K^2 h^{4/3}}, \tag{9}$$

where F_L is the Lorentz's linearization of the friction term (Lorentz, 1926). Cai et al. (2012a) determined a hybrid expression for tidal damping by following the envelope method (see: Savenije, 2012; pp. 59-61) and considering the new friction term (8), leading to a revised damping equation:

$$\delta = \frac{\mu^2}{1+\mu^2}\left(\gamma - \frac{2}{3}\chi\mu^2\lambda^2 - \frac{8}{9\pi}\chi\mu\lambda\right). \tag{10}$$

Equation (10), when combined with the phase lag equation, the scaling equation and the celerity equation forms a set of four implicit equations with four unknowns. Savenije et al. (2008) derived the phase lag equation as:

$$\tan(\varepsilon) = \frac{\lambda}{\gamma - \delta}, \tag{11}$$

the scaling equation as:

$$\mu = \frac{\sin(\varepsilon)}{\lambda} = \frac{\cos(\varepsilon)}{\gamma - \delta}, \tag{12}$$

and the celerity equation as:

$$\lambda^2 = 1 - \delta(\gamma - \delta). \tag{13}$$

Making use of the trigonometric equation $[\cos(\varepsilon)]^{-2} = 1 + [\tan(\varepsilon)]^2$, equations (11) and (12) can be combined to eliminate the variable ε to give:

$$(\gamma - \delta)^2 = \frac{1}{\mu^2} - \lambda^2. \tag{14}$$

The substitution of equations (10) and (13) into equation (14) results in:

$$\lambda^2\left[\delta\left(\mu^2-1\right)+\mu^2\left(\frac{1}{\lambda}-\lambda\right)\left(\frac{2}{3}\chi\mu^2\lambda+\frac{8}{9\pi}\chi\mu\right)\right]=0, \tag{15}$$

which can be simplified for $\lambda \neq 0$. Subsequently, equations (15) and (9) can be combined to yield a simple relationship between δ and μ, λ:

$$\delta=\frac{\gamma}{2}-\frac{4}{9\pi}\frac{\chi\mu}{\lambda}-\frac{\chi\mu^2}{3}, \tag{16}$$

after which this equation can be solved for μ, using the celerity equation (13) and equation (14).

Figure 2 shows the variation of the dependent dimensionless parameters obtained with both the hybrid model and Savenije's model (Savenije et al., 2008) as a function of the estuary shape number γ for different values of the friction number χ. Unlike the discontinuous behaviour (i.e., with two families of solutions) and the transition towards a standing wave (i.e., the wave celerity approaching infinity) predicted by Savenije et al. (2008), the hybrid model provides a continuous solution in the transition zone of critical convergence (Jay, 1991) where γ is close to 2. This is important since it enables the hybrid model to be applicable in the zones where the convergence is bigger than the critical convergence. For a frictionless (χ=0) or an ideal (where friction balances convergence) estuary, both models are identical.

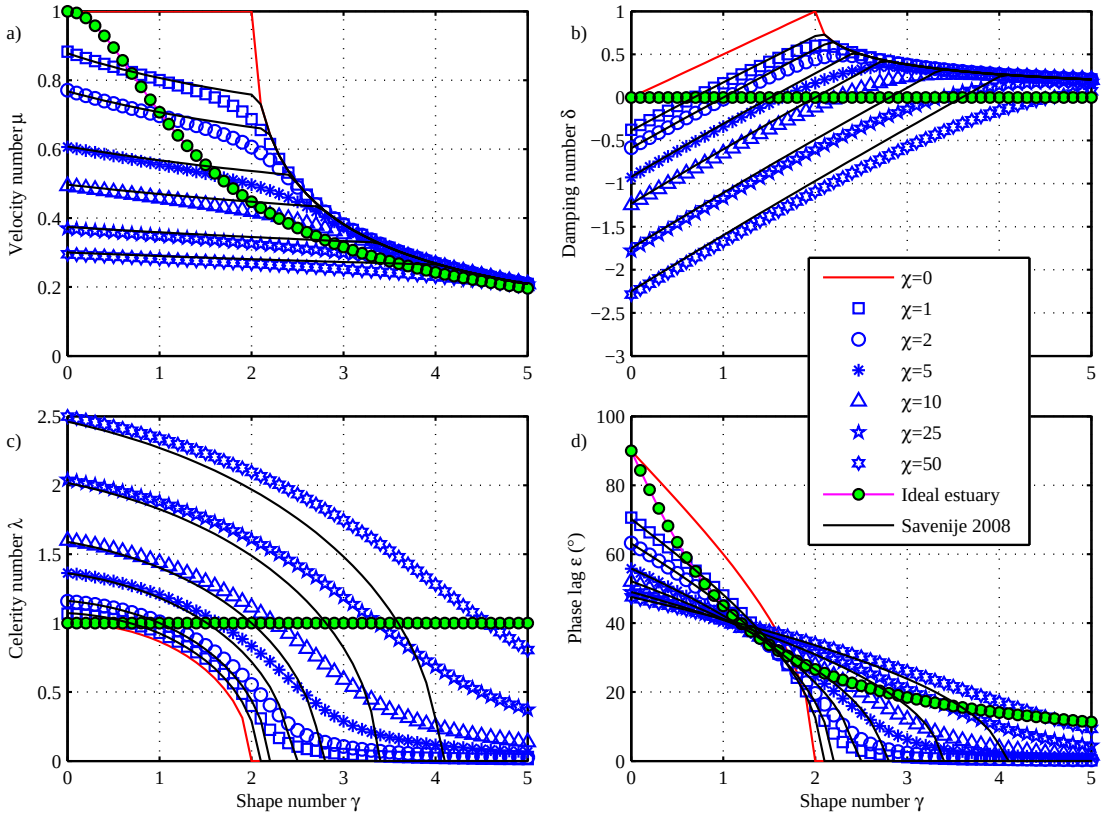

Figure 2. Relationship between the main dimensionless parameters (a: velocity number μ; b: damping number δ; c: celerity number λ; d: phase lag ε) and the estuary shape number γ for difference values of the friction number χ. The blue symbols represent the hybrid model, while the drawn black lines represent the solutions obtained by Savenije et al. (2008). The drawn red lines indicate the frictionless estuary (χ=0). The green round symbols indicate the ideal estuary.

3.2. *Hybrid model accounting for river discharge*

In the following, we extend the validity of the damping equation (9) by introducing the effect of river discharge in the friction term. For this purpose we introduce the dimensionless river discharge term φ:

$$\varphi = \frac{U_r}{\upsilon}, \tag{17}$$

which represents the landward boundary condition.

The development of the Lorentz's linearization of the friction term accounting for the effect of river discharge reads (Dronkers, 1964; pp. 272-275):

$$F_L = \frac{1}{K^2 h^{4/3}}\left(\frac{1}{4}L_0\upsilon^2 + \frac{1}{2}L_1\upsilon U_t\right), \tag{18}$$

where the expressions of coefficients L_0 and L_1 when $0 < \varphi < 1$ are:

$$L_0 = \left[2+\cos(2\alpha)\right]\left(2-\frac{4\alpha}{\pi}\right)+\frac{6}{\pi}\sin(2\alpha), \tag{19}$$

$$L_1 = \frac{6}{\pi}\sin(\alpha)+\frac{2}{3\pi}\sin(3\alpha)+\left(4-\frac{8\alpha}{\pi}\right)\cos(\alpha). \tag{20}$$

with

$$\alpha = \arccos(-\varphi), \tag{21}$$

where $\pi/2 < \alpha < \pi$ because $-\varphi$ is negative. If the river discharge is negligible, i.e., $U_r = 0$ and $\alpha = \pi/2$, equation (18) reduces to the classical Lorentz's linearization $L_0 = 0$ and $L_1 = 16/(3\pi)$.

When $\varphi \geq 1$,

$$L_0 = -2 - 4\varphi^2, \quad L_1 = 4\varphi. \tag{22}$$

If $\alpha = \pi$ is introduced into equations (19) and (20), then the same values follow as in (22), in the case of $\varphi = 1$ (i.e., $U_r = \upsilon$).

Consequently, the new hybrid friction term accounting for the effect of river discharge, with the same weights as in (9), reads:

$$F_H = \frac{1}{3}F_L + \frac{2}{3}F = \frac{1}{3}\frac{1}{K^2 h^{4/3}}\left(\frac{1}{4}L_0\upsilon^2 + \frac{1}{2}L_1\upsilon u_t\right)+\frac{2}{3}\frac{U|U|}{K^2 h^{4/3}}. \tag{23}$$

Using the friction formulation (23) for the derivation of the damping equation by subtracting the HW and LW envelopes, we are able to end up with the new damping equation:
in the downstream tide-dominated zone, where $\varphi < \mu\lambda$,

$$\frac{1}{\eta}\frac{\mathrm{d}\eta}{\mathrm{d}x}\left(\theta - r_s\frac{\varphi}{\sin(\varepsilon)}\zeta + \frac{g\eta}{c\upsilon\sin(\varepsilon)}\right) = \frac{\theta}{a} - f\frac{\upsilon}{\overline{h}c}\left(\frac{2}{3}\sin(\varepsilon)+\frac{16}{9}\varphi\zeta+\frac{2}{3}\frac{\varphi^2}{\sin(\varepsilon)}+\frac{L_1}{6}-\frac{L_0}{9}\frac{\zeta}{\sin(\varepsilon)}\right), \tag{24}$$

in the upstream river discharge-dominated zone, where $\varphi \geq \mu\lambda$,

$$\frac{1}{\eta}\frac{\mathrm{d}\eta}{\mathrm{d}x}\left(\theta - r_s\frac{\varphi}{\sin(\varepsilon)}\zeta + \frac{g\eta}{c\upsilon\sin(\varepsilon)}\right) = \frac{\theta}{a} - f\frac{\upsilon}{hc}\left(\frac{8}{9}\zeta\sin(\varepsilon) + \frac{4}{3}\varphi + \frac{8}{9}\frac{\varphi^2}{\sin(\varepsilon)}\zeta + \frac{L_1}{6} - \frac{L_0}{9}\frac{\zeta}{\sin(\varepsilon)}\right), \quad (25)$$

where θ is a correction factor for wave celerity defined as:

$$\theta = 1 - \left(\sqrt{1+\zeta} - 1\right)\frac{\varphi}{\mu\lambda}, \quad (26)$$

which is the dimensionless term that takes into account the fact that the wave celerity is not equal at HW and LW.

Making use of the dimensionless parameters defined in Table 1, equations (24) and (25) reduce to the following set of equations:

$$\begin{cases} \delta = \dfrac{\mu^2}{\mu^2\left[\theta - r_s\varphi\zeta/(\mu\lambda)\right]+1}\left[\gamma\theta - \chi\left(\dfrac{2}{3}\varphi^2 + \dfrac{16}{9}\mu\lambda\varphi\zeta + \dfrac{2}{3}\mu^2\lambda^2 + \dfrac{1}{6}L_1\mu\lambda - \dfrac{1}{9}L_0\zeta\right)\right] & (\varphi < \mu\lambda) \\ \delta = \dfrac{\mu^2}{\mu^2\left[\theta - r_s\varphi\zeta/(\mu\lambda)\right]+1}\left[\gamma\theta - \chi\left(\dfrac{8}{9}\varphi^2\zeta + \dfrac{4}{3}\mu\lambda\varphi + \dfrac{8}{9}\mu^2\lambda^2\zeta + \dfrac{1}{6}L_1\mu\lambda - \dfrac{1}{9}L_0\zeta\right)\right] & (\varphi \geq \mu\lambda) \end{cases}, \quad (27)$$

With equation (27) to replace equation (16), an analytical model can be made to assess the effect of river discharge on tidal damping and propagation. A fully explicit solutions for the main dimensionless parameters (i.e., μ, δ, λ, ε) cannot be derived, thus an iterative refinement is needed to obtain the correct wave behaviour. The following procedure usually converges in a few steps: (1) initially we assume Q_f=0 and calculate the initial values for the velocity number μ, celerity number λ and the tidal velocity amplitude (and hence dimensionless river discharge term φ) using the analytical solution proposed in Cai et al. (2012a); (2) taking into account the effect of river discharge Q_f, the revised damping number δ, velocity number μ, celerity number λ and velocity amplitude υ (and hence φ) are calculated by solving equations (27), (13), and (14) using a simple Newton-Raphson's method; (3) this process is repeated until the result is stable and then the other parameters (e.g., ε, η, υ) are computed.

Figure 3 presents the variation of the main dimensionless parameters (i.e., the damping number δ, the velocity number μ, the celerity number λ and the phase lag ε) with the estuary shape number γ for different river discharge conditions φ and for given values of ζ=0.1, χ=2 and r_s=1. It is evident from equation (27) that the influence of river discharge on the tidal dynamics is very similar to that of the friction number χ. In fact, the new friction term in the damping equation (27) can be rewritten as:

$$\begin{cases} \chi\left(\dfrac{2}{3}\varphi^2 + \dfrac{16}{9}\mu\lambda\varphi\zeta + \dfrac{2}{3}\mu^2\lambda^2 + \dfrac{1}{6}L_1\mu\lambda - \dfrac{1}{9}L_0\zeta\right) = \\ \dfrac{2}{3}\chi\mu^2\lambda^2\left(\dfrac{\varphi^2}{\mu^2\lambda^2} + \dfrac{8}{3}\dfrac{\varphi\zeta}{\mu\lambda} + 1\right) + \dfrac{8}{9\pi}\chi\mu\lambda\left(\dfrac{3\pi}{16}L_1 - \dfrac{\pi}{8}\dfrac{L_0\zeta}{\mu\lambda}\right) \quad (\varphi < \mu\lambda) \\ \chi\left(\dfrac{8}{9}\varphi^2\zeta + \dfrac{4}{3}\mu\lambda\varphi + \dfrac{8}{9}\mu^2\lambda^2\zeta + \dfrac{1}{6}L_1\mu\lambda - \dfrac{1}{9}L_0\zeta\right) = \\ \dfrac{2}{3}\chi\mu^2\lambda^2\left(\dfrac{4}{3}\dfrac{\varphi^2\zeta}{\mu^2\lambda^2} + 2\dfrac{\varphi}{\mu\lambda} + \dfrac{4}{3}\zeta\right) + \dfrac{8}{9\pi}\chi\mu\lambda\left(\dfrac{3\pi}{16}L_1 - \dfrac{\pi}{8}\dfrac{L_0\zeta}{\mu\lambda}\right) \quad (\varphi \geq \mu\lambda) \end{cases}, \quad (28)$$

which shows that the effect of river discharge is basically that of increasing friction by a factor, as a function of the dimensionless river discharge φ (i.e., by comparing the right-hand side of equation (28) with the last two terms in equation (10)). In general, the damping number and the velocity number decrease with river discharge, which means more tidal damping and less velocity amplitude. On the other hand, the celerity number is increased (hence slower wave celerity) due to the increasing river discharge. For the phase lag, we can see from Figure 3d that it decreases with river discharge for small values of γ while it is

increased for bigger values of γ. Cai et al. (2012a) found very similar trends between the main dimensionless parameters and the friction number χ, which confirms our point that the effect of river discharge acts in the same way as increasing or decreasing the friction.

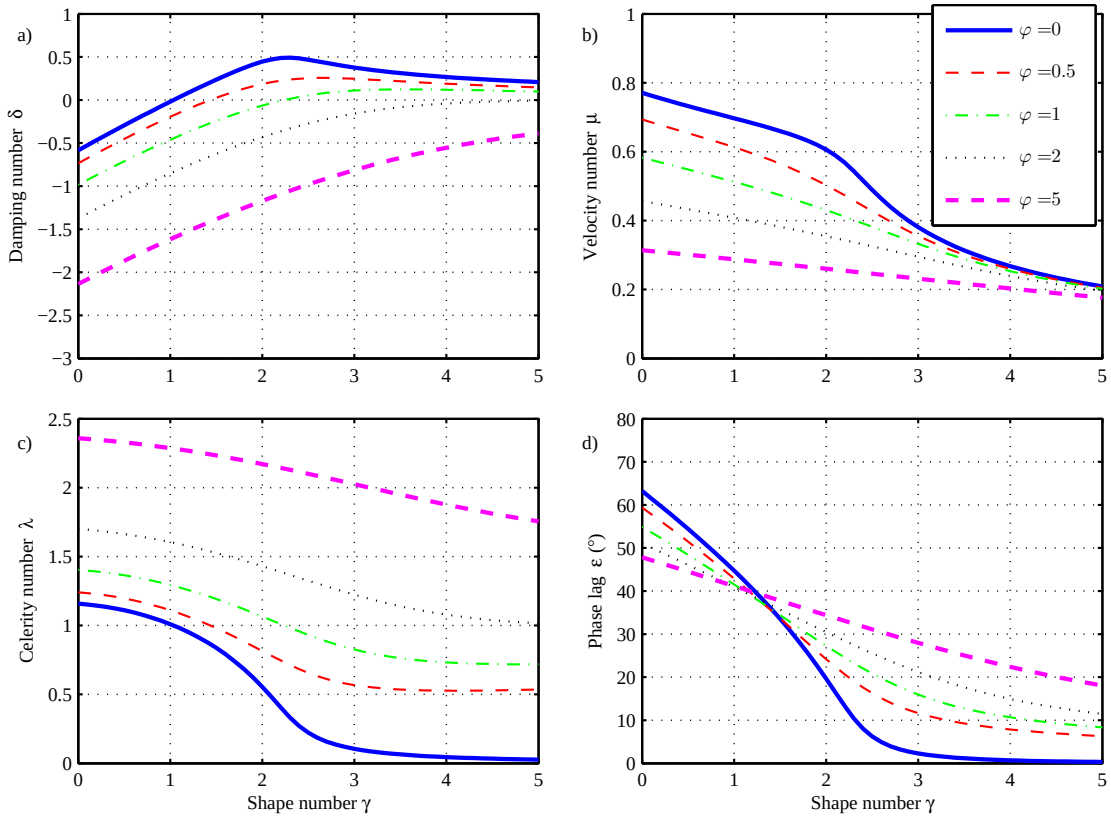

Figure 3. Relationships between the main dimensionless parameters and the estuary shape number γ obtained by solving the equations (27), (13) and (14) for different values of the dimensionless river discharge term φ with ζ=0.1, χ=2 and r_s=1.

4. Application to the Modaomen estuary

4.1 *Calibration and verification*

The Modaomen estuary, which has the largest flood discharge and sediment transport rate in the Pearl River Delta in China, has been significantly affected by human activities (e.g., dredging, flow reduction). In recent years, severe salt intrusion has threatened the freshwater supply in this area during the dry season, which is due to the change of tidal dynamics. The proposed analytical model provides an increased understanding of tidal wave propagation in estuaries and could be used as a tool for assessing the effect of these human interventions on tidal dynamics.

With the new damping equation (27), an analytical model can be developed and compared to observations made in the Modaomen estuary. Table 2 presents the geometry and flow characteristics (used for both model calibration and verification) of the Modaomen on which the computations are based. The convergence length of the cross-sectional area, which is the length scale of the exponential function, is obtained by calibration of equation (1), where the parallel branches separated by islands have been combined, as suggested by Nguyen and Savenije (2006) and Zhang et al. (2012).

The observations of tidal amplitude and travel time at HW and LW along the Modaomen estuaries on 8-9 February 2001 have been used to calibrate the model, while the observed data on 5-6 December 2002 were used for verification. The calibrated parameters, i.e. the storage width ratio r_s and the Manning-Strickler friction K, are presented in Table 3. In general, the storage width ratio r_s ranges between 1 and 2

(Savenije; p. 21), while the Manning-Strickler friction K in estuaries typically varies within a range of between 17 and 60 $m^{1/3}s^{-1}$ (Cai et al., 2012b).

Table 2. Geometric and flow characteristics of the estuary studied in two different periods (used for calibration and verification, respectively).

Estuary	Reach (km)	Depth $\overline{h}$ (m)	Convergence length a (km)	Cross-sectional area $\overline{A_0}$ (m^2)	Tidal amplitude at the mouth (m)		River discharge Q_f (m^3s^{-1})	
					Calibration	Verification	Calibration	Verification
Modaomen	0~43	5.5~6.3	106	9,300	1.31	1.09	2,259	2,570
	43~91	7.1~8.2	inf					
	91~150	10.3	110					

Table 3. Calibrated parameters of the estuary studied considering the explicit effect of river discharge.

Estuary	Reach (km)	Storage width ratio r_S (-)	Manning-Strickler friction K ($m^{1/3}s^{-1}$), Q_f >0
Modaomen	0~43	1.1	29
	43~91	1.1	56
	91~150	1	56

Both the models with and without river discharge could be made to fit the observations if a suitable friction coefficient is used. However, calibration without river discharge would result in significantly different (and unrealistic) values of the Manning-Strickler coefficients in the upstream part of the estuaries. For example, we would have arrived at K=19 $m^{1/3}s^{-1}$ for the model that does not take account of river discharge in the upstream part of Modaomen estuary (91~150 km).

Figure 4 shows the longitudinal computation of the tidal amplitude, the travel time (HW, LW) and the dimensionless damping number applied to the Modaomen estuary. The new model accounting for the effect of river discharge is compared to the original model with the same K as in Table 3, but without river discharge. As can be seen from the variation of the dimensionless damping number (Figure 4cf), in the downstream end of the estuary the models are almost identical, but perform differently in the upper reach where the effect of river discharge is more strongly felt. It can be seen that without considering the river discharge, the model substantially underestimates the tidal damping in the upstream part of the estuaries.

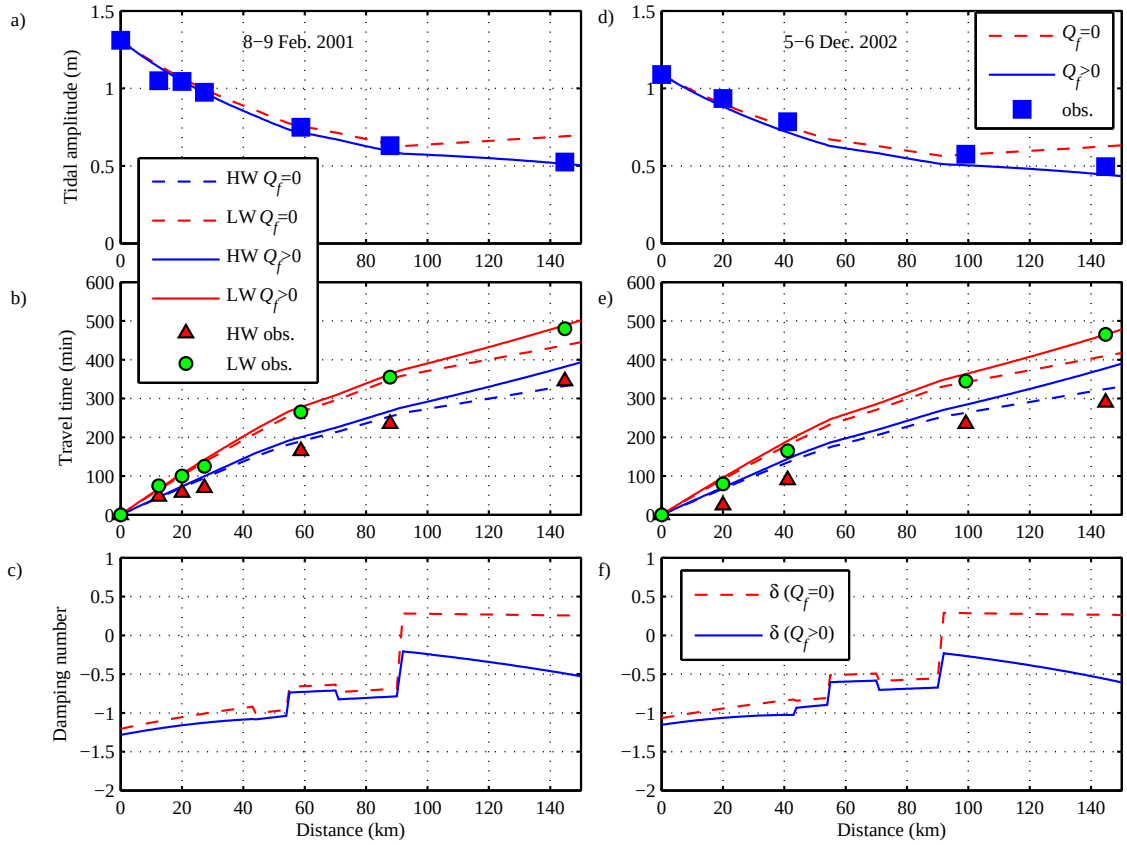

Figure 4. Comparison of analytically calculated tidal amplitude (a, d), travel time (b, e) with measurements and comparison of two analytical models to compute the dimensionless damping number (c, f) on 8-9 February 2001 and 5-6 December 2002 in the Modaomen estuary. The dashed line represents the model where river discharge is neglected. The continuous line represents the model accounting for the effect of river discharge. Both models used the same friction coefficients calibrated with the model considering the river discharge (see Table 3).

4.2 *The sensitivity to river discharge*

To demonstrate a practical application of the proposed analytical solution, the model has been used to assess the effect of river charge on tidal dynamics in the Modaomen estuary. It should be noted that all the calibration parameters (including the friction coefficient K and storage width ratio r_S) are fixed for the sensitivity experiments. Taking the spring tide on February 8-9, 2001 with the same tidal amplitude at the estuary mouth as the baseline, the longitudinal variation of tidal amplitude, travel time for HW and LW, velocity amplitude and phase lag under different river discharge conditions is presented in Figure 5. We can see that the tidal damping increases with river discharge. In particular, the tidal amplitude, the wave celerity (HW and LW) , the velocity amplitude and phase lag are decreased with increasing river discharge. However, it is important to note that the largest effect is in the upstream part of the estuary, where the estuary gradually becomes more riverine in character (i.e., from 90 km onwards). The reason can be attributed to the friction term $\frac{2}{3}\chi\mu^2\lambda^2\left(\frac{4}{3}\frac{\varphi^2\zeta}{\mu^2\lambda^2}+2\frac{\varphi}{\mu\lambda}+\frac{4}{3}\zeta\right)+\frac{8}{9\pi}\chi\mu\lambda\left(\frac{3\pi}{16}L_1-\frac{\pi}{8}\frac{L_0\zeta}{\mu\lambda}\right)$ in the new damping equation (see (28)) for the upstream part of the estuary ($\varphi\geq\mu\lambda$), which is more sensitive to river discharge. Furthermore, it can be seen from Figure 5d that the influence of river discharge on phase lag is minor in the Modaomen estuary.

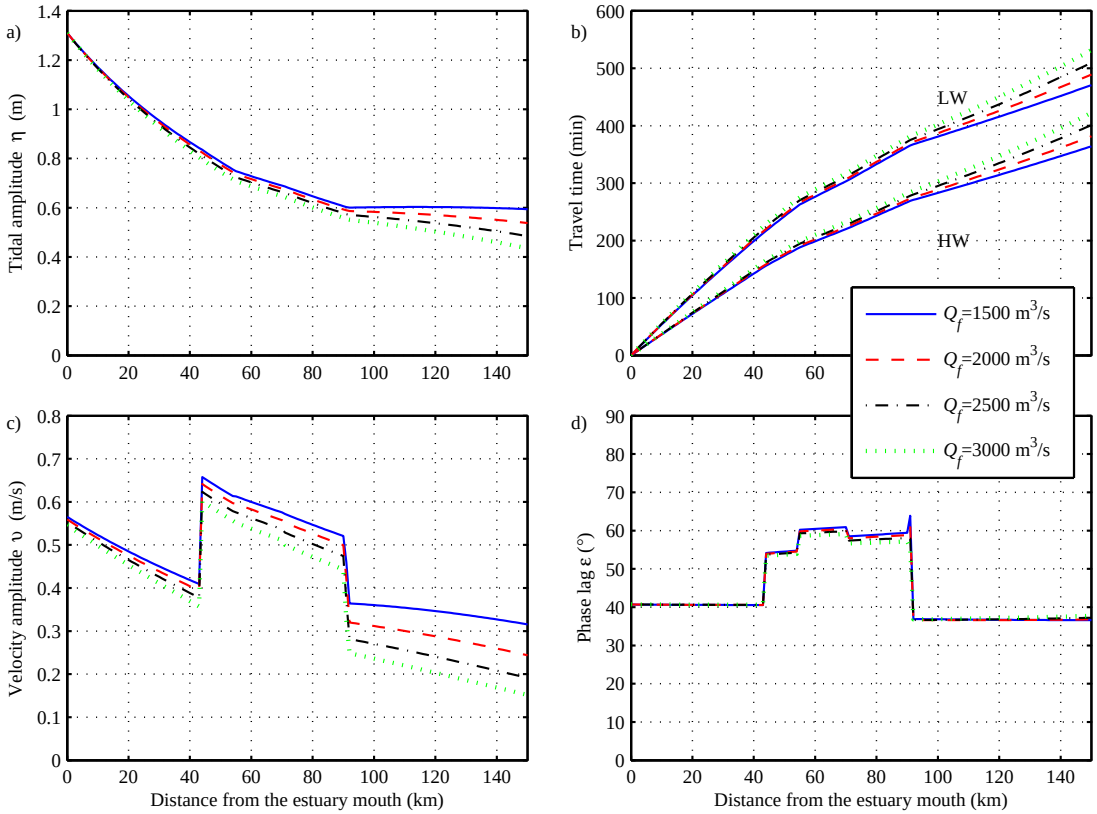

Figure 5. Longitudinal variation of the tidal amplitude (a), travel time of HW and LW (b), tidal velocity amplitude (c) and phase lag (d) in the Modaomen estuary under different river discharge conditions.

5. Conclusions

In this paper, we analyzed the effect of river discharge on tidal propagation in the Modaomen estuary. The influence of river discharge on tidal dynamics is considerable, especially in the upstream part of the estuary where the river discharge is largely responsible for the considerable tidal damping. It is demonstrated that river discharge is felt primarily through the friction term. The results show that the proposed model fits the observations with realistic roughness value in the upstream part of the estuary, while the model with negligible river discharge can only be fitted with unrealistically high roughness values. Moreover, as illustrated in the Modaomen estuary, the proposed analytical model can be a useful and accurate tool to assess the effect of human interventions (e.g., freshwater withdrawn along the estuary) on tidal dynamics. In addition, it is worth noting that the analytical model is particularly useful when combined with ecological or salt intrusion models where it can provide essential tidal parameters (e.g., velocity amplitude, wave celerity and tidal damping/amplification).

Acknowledgements

The first author is financially supported during his PhD program by the China Scholarship Council with the project reference number of 2010638037.

References

Buschman, F.A., Hoitink, A.J.F., van der Vegt, M. and Hoekstra, P., 2009. Subtidal water level variation controlled by

river flow and tides, *Water Resources Research*, 45, W10420, doi: 10.1029/2009WR008167.
Cai, H., H. H. G. Savenije and M. Toffolon, 2012a. A new analytical framework for assessing the effect of sea-level rise and dredging on tidal damping in estuaries, *Journal of Geophysical Research*, 117, C09023, doi:10.1029/2012JC008000.
Cai, H., Savenije, H.H.G., Yang, Q., Ou, S. and Lei, Y., 2012b. Influence of River Discharge and Dredging on Tidal Wave Propagation: Modaomen Estuary Case, *Journal of Hydraulic Engineering-Asce*, 138(10), 885-896, doi: 10.1061/(ASCE)HY.1943-7900.0000594.
Cai, H., H. H. G. Savenije and M. Toffolon, 2013. The effect of river discharge on tidal damping in estuaries: a comparative analysis of friction formulations, *Journal of Geophysical Research*, to be submitted.
Dronkers, J.J., 1964. *Tidal Computations in Rivers and Coastal Waters*. North-Holland Publishing Company, Amsterdam.
Godin, G., 1985. Modification of River Tides by the Discharge, *Journal of Waterway Port Coastal and Ocean Engineering-Asce*, 111(2): 257-274.
Godin, G., 1999. The propagation of tides up rivers with special considerations on the upper Saint Lawrence river, *Estuarine Coastal and Shelf Science*, 48(3): 307-324.
Horrevoets, A. C., H. H. G. Savenije, J. N. Schuurman and S. Graas, 2004. The influence of river discharge on tidal damping in alluvial estuaries, *Journal of Hydrology*, 294(4): 213-228.
Jay, D. A., 1991. Green Law Revisited - Tidal Long-Wave Propagation in Channels with Strong Topography, *Journal of Geophysical Research*, 96(C11), 20585-20598.
Jay, D.A., Leffler, K. and Degens, S., 2011. Long-Term Evolution of Columbia River Tides, *Journal of Waterway Port Coastal and Ocean Engineering-Asce*, 137: 182-191.
Kukulka, T. and D. A. Jay, 2003. Impacts of Columbia River discharge on salmonid habitat: 1. A nonstationary fluvial tide model, *Journal of Geophysical Research*, 108(C9).
Leblond, P. H., 1978. Tidal Propagation in Shallow Rivers, *Journal of Geophysical Research-Oceans and Atmospheres*, 83(Nc9): 4717-4721.
Lorentz, H. A., 1926. *Verslag Staatscommissie Zuiderzee*, Algemene Landsdrukkerij, The Hague, Netherlands.
Nguyen, A. D. and Savenije, H. H. G., 2006. Salt intrusion in multi-channel estuaries: a case study in the Mekong Delta, Vietnam, *Hydrology and Earth System Sciences*, 10(5): 743-754.
Savenije, H. H. G., 1998. Analytical expression for tidal damping in alluvial estuaries, *Journal of Hydraulic Engineering-Asce*, 124(6): 615-618.
Savenije, H. H. G., 2001. A simple analytical expression to describe tidal damping or amplification, J Hydrol, 243(3-4), 205-215.
Savenije, H.H.G., 2005. *Salinity and Tides in Alluvial Estuaries*, Elsevier, New York.
Savenije, H.H.G., 2012. *Salinity and Tides in Alluvial Estuaries*, 2nd completely revised edition, http://salinityandtides.com.
Savenije, H. H. G., M. Toffolon, J. Haas, and E. J. M. Veling, 2008. Analytical description of tidal dynamics in convergent estuaries, *Journal of Geophysical Research*, 113, C10025, doi:10.1029/2007JC004408.
Toffolon, M. and H. H. G. Savenije, 2011. Revisiting linearized one-dimensional tidal propagation, *Journal of Geophysical Research*, 116, C07007, doi:10.1029/2010JC006616.
Toffolon, M., Vignoli, G. and Tubino, M., 2006. Relevant parameters and finite amplitude effects in estuarine hydrodynamics, *Journal of Geophysical Research*, 111, C10014, doi:10.1029/2005JC003104.
van Rijn, L. C., 2011. Analytical and numerical analysis of tides and salinities in estuaries; part I: tidal wave propagation in convergent estuaries, *Ocean Dynamics*, 61(11): 1719-1741.
Zhang, E. F., Savenije, H. H. G., Chen, S. L. and Mao, X. H., 2012. An analytical solution for tidal propagation in the Yangtze Estuary, China, *Hydrology and Earth System Sciences*, 16: 3327-3339, doi:10.5194/hess-16-3327-2012.